UNIVERSITÀ
DEGLI STUDI
DI PADOVA

DIPARTIMENTO
DI INGEGNERIA
DELL'INFORMAZIONE

DIPARTIMENTO DI INGEGNERIA DELL'INFORMAZIONE

CORSO DI LAUREA IN INGEGNERIA DELL'INFORMAZIONE

"STATE SPACE OBSERVERS AND CONTROLLERS FOR A TAKE-HOME MAGNETIC LEVITATION SYSTEM"

Relatore: Prof. Damiano Varagnolo
Università degli studi di Padova

Laureando: Andrea Nicetto

Correlatore: PhD(c) Hans A. Engmark
NTNU: Norwegian University of Science and Technology

ANNO ACCADEMICO 2021 – 2022

Data di laurea 14 Novembre 2022

Abstract

We consider a magnetic levitation system intended to become a take-home laboratory for learning control engineering concepts.

We thus assume the hardware specifics as given, and focus on the software part; more specifically, on developing control algorithms and a state space estimation strategy that extend and improve the classical model free approaches such as Proportional, Integral and Derivative (PID) control.

The first part of the thesis is dedicated to the design, implementation and testing of a Linear Quadratic Regulator whose aim is to adjust the vertical position of the levitating component and reject small disturbances. This LQR controller is based once again on the linearized dynamics of the model of the system.

The second part of this work focuses thus on designing, implementing, tuning and testing a Kalman filter that returns an estimate for the vertical and horizontal position of the levitating magnet, based on Hall sensors measurements and a linearized dynamics used for the development of the LQR above.

Through a series of experiments it is shown that the LQR controller is able to stabilise the system if the levitating magnet starts from a position close to the equilibrium point. Moreover, it is displayed that the implemented Kalman filter is able to accurately estimate the states of the nonlinear system model, indeed corroborating the idea of its usefulness in estimating the states of the real system.

Abstract

In questa tesi di laurea triennale viene considerato un sistema di levitazione magnetica destinato a essere un laboratorio da portare a casa per l'apprendimento dei concetti di ingegneria del controllo.

Dato il sistema hardware, il progetto si dedica alla parte software; più precisamente, allo sviluppo di algoritmi di controllo e di stima dello spazio di stato che estendono e migliorano gli approcci classici come il controllo Proporzionale, Integrale e Derivativo (PID).

La prima parte della tesi è dedicata alla progettazione, all'implementazione e al collaudo di un regolatore lineare quadratico il cui scopo è regolare la posizione verticale del componente levitante e respingere piccoli disturbi. Questo regolatore LQR si basa ancora una volta sulla dinamica linearizzata del modello del sistema.

La seconda parte di questo lavoro si concentra quindi sulla progettazione, l'implementazione, e il collaudo di un filtro di Kalman che restituisce una stima della posizione verticale e orizzontale del magnete levitante, basata sulle misure dei sensori di Hall e su una dinamica linearizzata utilizzata per lo sviluppo del LQR di cui sopra.

Attraverso una serie di esperimenti si dimostra che il controllore LQR è in grado di stabilizzare il sistema se il magnete levitante parte da una posizione vicina al punto di equilibrio. Inoltre, si osserva che il filtro di Kalman implementato è in grado di stimare accuratamente gli stati del modello di sistema non lineare, avvalorando di fatto l'idea della sua utilità nella stima degli stati del sistema reale.

Contents

List of Figures

List of Tables

Chapter 1

Introduction

Magnetic levitation (maglev) or magnetic suspension is a method by which an object is suspended with no support other than magnetic fields. Magnetic force is used to counteract the effects of the gravitational force and any other forces. Magnetic levitation is used for maglev trains, contactless melting, magnetic bearings and for product display purposes. The two primary issues involved in magnetic levitation are lifting forces: providing an upward force sufficient to counteract gravity, and stability: ensuring that the system does not spontaneously slide or flip into a configuration where the lift is neutralized.

These principles were analysed in this paper on the basis of the project handled by a group of students from The Norwegian University of Science and Technology (NTNU). Specifically, the design consists of a magnetic disc that levitates above a base of neodymium magnets and solenoids that are current-carrying.

Everything was done in simulation after modelling the various components within the Matlab environment where an attempt was made to apply a LQR controller and a Kalman filter capable of estimating the states of the system.

The aim is to try to improve the performance obtained using a classical model free approach such as PID.

1.1 Overview of the report

The thesis is divided into 7 chapters.

The first chapter is a brief introduction to the subject, including information on magnets and various applications of magnetic levitation.

The second chapter aims to provide the theoretical framework required to understand the subject. It includes relevant theoretical topics such as the magnetic field, the physical forces associated with it, the Linear Quadratic Regulator and the Kalman filter in the continuous case.

The third chapter deals with the system description and the mathematical model adopted to study the system.

The fourth chapter focuses on how the mathematical model and the various physical components were implemented within the Matlab environment. It also shows how the equilibrium point of the system around which the controller will be applied was calculated.

The fifth chapter shows how the system was linearised around the equilibrium point and how the LQR controller was applied. It also discusses the results obtained from simulations based on different starting points of the levitating component.

The sixth chapter is about the Kalman filter design and how well it is able to estimate the states of the nonlinear system.

Finally, the seventh chapter examines the results of the controller and filter and discusses some future improvements that could be applied to the project.

Chapter 2

Theoretical framework

The purpose of this chapter is to provide the theoretical framework needed. The chapter includes various theorems and physical laws that are relevant to the project.

2.1 Earnshaw's theorem

One of the most essential theorems in the magnetic levitation industry, is a theorem presented by Samuel Earnshaw in 1840. The theorem states that "no system of charged particles can be in stable static equilibrium in the absence of external forces" (Jones 1980).
This essentially means that it is not possible to keep the levitating magnet stable, only by the static magnetic field from permanent magnets. The levitating magnet needs some form of stabilizing force, which in this project is provided by four solenoids. The goal is therefore to control the current flowing through each solenoid in order to create a stable equilibrium for the levitating magnet.

2.2 Biot-Savart's law

Biot-Savart's law is generally an equation that describes the magnetic field generated by a current. More specifically it computes the magnetic field B at a position

r in a 3D space, generated by a constant current I:

$$B(r) = \frac{\mu_0}{4\pi} \int_C \frac{I d\ell \times r'}{|r'|^3} \tag{2.1}$$

Where I is the current in a wire, $d\ell$ is a differential vector along the line C (wire), μ_0 is the permeability of air, C is the wire and r' is the point at which the magnetic field is being computed. r' corresponds to $p - l$, where p is a point in Cartesian coordinates and l is the point on the line C (wire).

2.3 Laplace's force

Laplace's force law is a law derived from Lorentz force law. Laplace's force law states the net magnetic force on a stationary and rigid curved wire that carries a steady current. This is given by:

$$F_b = I \int_C d\ell \times B \tag{2.2}$$

Where F_b is the magnetic force, I is the current, $d\ell$ is an infinitesimal segment of the wire C, and B is the magnetic field.

2.4 Permanent magnet

A permanent magnet is a magnet in which the magnetic field originates from the internal material of the magnet itself. The magnetic field generated from the magnet is permanent, meaning it can never be turned off as in a solenoid. The magnets used in this project are neodymium magnets, which are made of an alloy of neodymium, iron and boron. This is the strongest type of permanent magnet in the world as of today (Fraden 2010) [9].

The magnetic field from a permanent magnet are most vertical near the poles. A simulation of the magnetic field around a neodymium magnet is shown in figure 2.1. The gray box in the middle is a stack of 3 neodymium magnets, shown from the side. The blue vector field represents a cross section of the magnetic field, shown in the yz-axis.

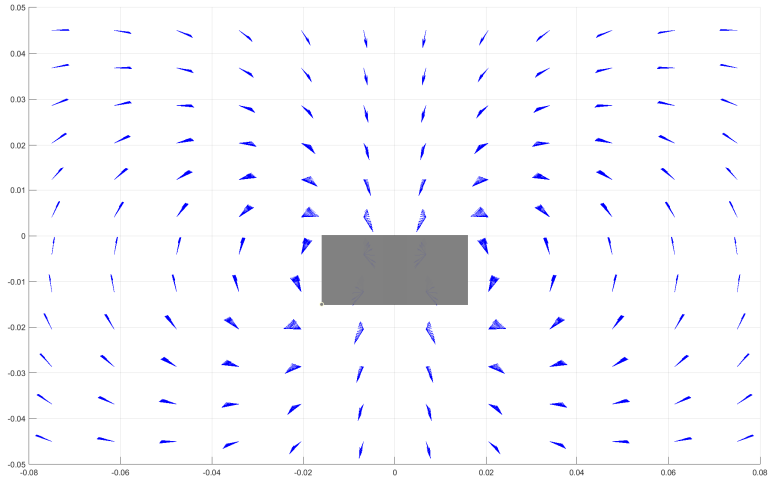

Figure 2.1: Illustration of the magnetic field generated by a permanent magnet

2.5 Solenoids

A solenoid is a type of electromagnet. It consists of a coiled cylindrical copper wire, which gets magnetized when current flows through it. The difference between an electromagnet and a solenoid, is the core. An electromagnet has a core of magnetic material, e.g. iron, which becomes magnetized when current flows through the wire. A solenoid has the same coil of wires, but not a core that can be magnetized. Figure 2.2 is an illustration of the magnetic field generates by a current I, flowing through the coil of wire. N and S are the north and south pole of the generated magnetic field.

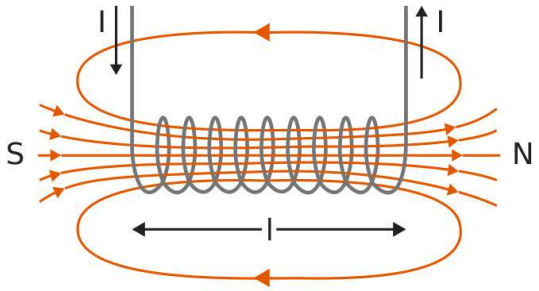

Figure 2.2: Magnetic field of a solenoid

2.6 Magnetic permeability

Magnetic permeability is the physical aspect of the magnetization certain materials obtain when being exposed to a magnetic field. In electromagnetism this has an impact on the strength of the magnetic field, in regards of different materials used in the core. An electromagnet that has a low permeability core has a lower magnetic field strength compared to the same electromagnet with a higher permeability in the core. An example of an electromagnet with a low permeability core is a solenoid, which can use air or plastic in the core. This has a lower magnetic field strength than a coil using an iron- or stainless steel core. This also has an impact on the inductance. The greater the permeability, the greater the inductance of an electromagnet. This effects the time constant, τ , of the coil. The formula for τ is shown in equation 2.3, and consists of the inductance L divided by the resistance R.

$$\tau = \frac{L}{R} \tag{2.3}$$

The electromagnets τ is the ability for the coils to reach 63% of its applied current. It takes 5τ for the coils to reach within $\pm 1\%$ of its final value.

2.7 LQR controller

The Linear Quadratic Regulator (LQR) is a method that provides optimally controlled feedback gains to enable the closed-loop stable and high performance design of systems. For continuous-time systems, the LQR computes the state-feedback control $u = -Kx$ that minimizes the quadratic cost function:

$$J(u) = \int_0^\infty \left(x^T Q x + u^T R u + 2x^T N u\right) dt \tag{2.4}$$

subject to the system dynamics $\dot{x} = Ax + Bu$.
Where $Q = Q^T \geq 0, R = R^T > 0$ are state cost and input cost matrices.
The resulting closed-loop system is:

$$\dot{x} = Ax + Bu = (A - BK)x \tag{2.5}$$

2.8 Kalman filter

The Kalman Filter is one of the most important and common estimation algorithms; it is used to estimate or predict the future evolution of hidden variables based on inaccurate and uncertain measurements.

The continuous time version of the Kalman Filter for the linear state space model

$$\begin{aligned} \frac{d}{dt}x(t) &= A(t)x(t) + B(t)u(t) + w(t) \\ z(t) &= H(t)x(t) + v(t) \end{aligned} \tag{2.6}$$

is give by

$$\begin{aligned} \frac{d}{dt}\hat{x}(t) &= A(t)\hat{x}(t) + B(t)u(t) + K(t)(z(t) - H(t)\hat{x}(t)) \\ \frac{d}{dt}P(t) &= A(t)P(t) + P(t)A^{\top}(t) + Q(t) - K(t)R(t)K^{\top}(t) \end{aligned} \tag{2.7}$$

where the Kalman gain is given by

$$K(t) = P(t)H^{\top}(t)R^{-1}(t) \tag{2.8}$$

Here $Q(t)$ and $R(t)$ represent the Power Spectral Density of the two white noise terms $w(t)$ and $v(t)$, respectively, $P(t)$ is the covariance of the estimated states and $K(t)$ is the Kalman gain.

Note that in this expression for $K(t)$ the covariance of the observation noise $R(t)$ also represents the covariance of the prediction error (or innovation) $\tilde{y}(t) = z(t) - H(t)\hat{x}(t)$.

An important part of successfully applying a Kalman Filter is that the states of the system need to be "observable". When a system is said to be observable it indicates that there is sufficient information about the states in the measurements of the system, i.e. it is possible to estimate the states accurately from the measurements. For a linear system, observability is checked by analysing the rank of the observability matrix

$$\mathcal{O} = \Big[H(t), \quad H(t)A(t), \quad \ldots, \quad H(t)A^{n-1}(t)\Big]^{T} \tag{2.9}$$

where n is the number of states in the system. If this matrix is full rank, then the system is observable.

Chapter 3

Mathematical model and system description

This chapter covers the mathematical foundation used to model the system and how it was applied to find a reasonable magnet configuration.

3.1 System description

A basic illustration of the magnetic levitation platform is shown in figure 3.1. There are 8 groups of permanent magnets (coloured in grey), placed in a circle centered on the platform with radius of 8.5cm, creating a permanent magnet field. The 4 Solenoids (coloured in red) are placed on a circle inside the permanent magnet circle with radius of 4.0cm. The combination of the permanent magnetic field and the controllable magnetic field from the solenoids should in theory make it possible to magnetically levitate a disc magnet (coloured in blue) in the air.

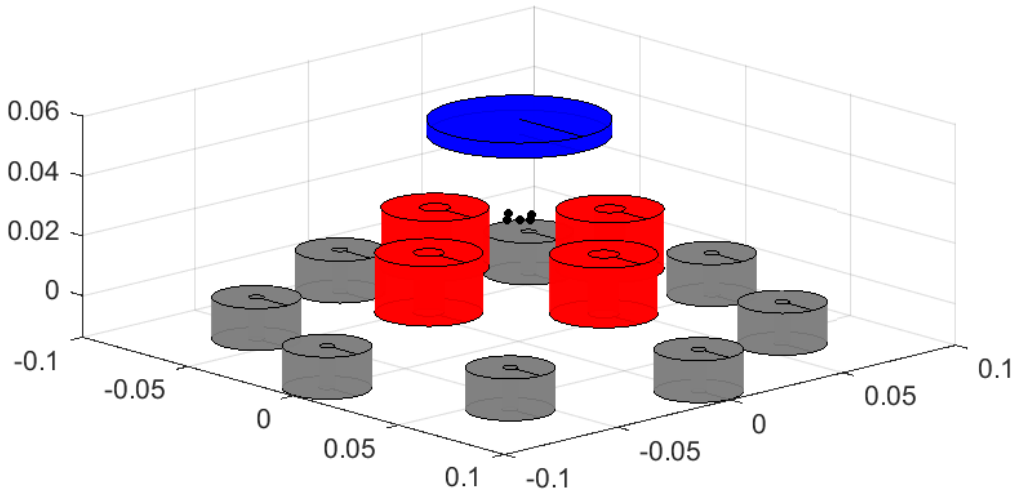

Figure 3.1: System illustration

3.2 Mathematical model

The mathematical model is based on the existing model described in the internal document "Model Description: Magnetic Levitation System" (Doshmanziari, Engmark and Hoang 2021), hereby referred to as the "Model description". The document models a magnetic levitation platform equivalent to the one used in this project by treating all the magnets involved as solenoids. The solenoids are modelled as thin wire loops. Using Biot-Savart's law and Laplace's force law it is possible to estimate the force from the solenoids on the levitating magnet based on the current in the wire loops. To make the approximation possible the loops are discretized into n = 100 linear segments. Also, in order to get a more accurate representation of the real magnetic field, the permanent magnets are instead modelled as separate solenoids, but with a set current.

The position and angle of the levitating magnet in relation to the coordinate frame in figure 3.1 is described by the state vector:

$$\eta = \begin{bmatrix} x_m & y_m & z_m & \psi_m & \theta_m & \varphi_m & \dot{x}_m & \dot{y}_m & \dot{z}_m & \dot{\psi}_m & \dot{\theta}_m & \dot{\varphi}_m \end{bmatrix}' \tag{3.1}$$

3.3 System equations

The model description also assumes full state feedback, which the system does not have. The measurements are instead the magnetic field in x,y and z direction, as measured by three hall-effect sensors placed in the positions:

$$\begin{aligned} p_x &= \begin{bmatrix} 0.0055 & -0.0055 & 0 & 0 & 0 \end{bmatrix}^T \\ p_y &= \begin{bmatrix} 0 & 0 & 0.0055 & -0.0055 & 0 \end{bmatrix}^T \\ p_z &= \begin{bmatrix} 0.0275 & 0.0275 & 0.0275 & 0.0275 & 0.0275 \end{bmatrix}^T \end{aligned} \tag{3.2}$$

Using Biot-Savart's law with the sensor positions as the points of interest the measurements can be described by the vector function $h(\eta, u)$. The model description presents the following simplification of Biot-Savart's law, as originally described in the paper from (Gonzalez and Cardenas 2020):

$$\begin{aligned} \mathbf{B}_\rho(\rho, z) = &\frac{\mu_0 I}{2\pi\sqrt{(\rho' + \rho)^2 + (z - z')^2}} \left\{ \frac{(z - z')}{\rho} \cdot \left[\frac{\rho'^2 + \rho^2 + (z - z')^2}{(\rho - \rho')^2 + (z - z')^2} E(k) - K(k) \right] \mathbf{e}_\rho \right. \\ &\left. - \left[\frac{\rho^2 - \rho'^2 + (z - z')^2}{(\rho - \rho')^2 + (z - z')^2} E(k) - K(k) \right] \mathbf{e}_z \right\} \\ k = &\frac{4\rho'\rho}{(\rho' + \rho)^2 + (z - z')^2} \end{aligned} \tag{3.3}$$

Where ρ' and z' are the radius and height of the wire loop. $K(k)$ and $E(k)$ are the elliptic integrals of the first and second kind. The limit case of when $\rho \to 0$ is also presented as:

$$\mathbf{B}_z = \frac{\mu_0 \rho'^2 I}{2\left[\rho'^2 + (z - z')^2\right]^{3/2}} \tag{3.4}$$

In order to calculate the magnetic field in a point using cartesian coordinates, $p = [x, y, z]^T$, the following equations are used.

$$\begin{aligned} \mathbf{B}_x(p) &= \mathbf{B}_\rho(\rho, z)\cos\phi \\ \mathbf{B}_y(p) &= \mathbf{B}_\rho(\rho, z)\sin\phi \\ \mathbf{B}_z(p) &= \mathbf{B}_z(\rho, z) \end{aligned} \tag{3.5}$$

Expanding the equations from the model description to include the permanent magnets we get:

$$h(\eta, u) = \overrightarrow{\mathbf{B}} = \sum_{i=1}^{m} \begin{bmatrix} B_x\left(p_x - p_s^i\right) \\ B_y\left(p_y - p_s^i\right) \\ B_z\left(p_z - p_s^i\right) \end{bmatrix} + \sum_{j=1}^{n} \begin{bmatrix} B_x\left(p_x - p_m^j\right) \\ B_y\left(p_y - p_m^j\right) \\ B_z\left(p_z - p_m^j\right) \end{bmatrix} \tag{3.6}$$

for a system with m solenoids and n permanent magnets, where p_s^i is the center of the i-th solenoid and p_m^j is the center of the j-th permanent magnet. p_x, p_y and p_z is the positions of the three hall effect sensors. The system can then be represented by the equations:

$$\begin{aligned} \dot{\eta} &= A\eta + B\phi(\eta, u) \\ y &= h(\eta, u) \end{aligned} \tag{3.7}$$

Where, like in the model description:

$$\begin{aligned} A &= \begin{bmatrix} O_{6x6} & I_6 \\ O_{6x6} & O_{6x6} \end{bmatrix} \\ B &= \begin{bmatrix} O_{6x6} \\ I_6 \end{bmatrix} \end{aligned} \tag{3.8}$$

and

$$\phi(\eta, u) = \begin{bmatrix} mI_3 & O_{3x3} \\ O_{3x3} & \mathcal{I} \end{bmatrix}^{-1} \begin{bmatrix} F_b(\eta, u) \\ \tau_b(\eta, u) \end{bmatrix} - \begin{bmatrix} O_{2x1} \\ g \\ O_{3x1} \end{bmatrix} \tag{3.9}$$

3.4 Equilibrium points

Analysing the equilibrium points is crucial for deciding where the system should be linearized so that the controller can be applied. The system is in equilibrium if:

$$\dot{\eta} = A\eta + B\phi(\eta, u) = 0 \tag{3.10}$$

Which for an autonomous system ($u = \mathbf{0}$) becomes:

$$\dot{\eta} = \begin{bmatrix} \dot{x}_m \\ \dot{y}_m \\ \dot{z}_m \\ \dot{\psi}_m \\ \dot{\theta}_m \\ \dot{\varphi}_m \\ F_x/m \\ F_y/m \\ F_z/m - g \\ \tau_\psi/\mathcal{I} \\ \tau_\theta/\mathcal{I} \\ \tau_\varphi/\mathcal{I} \end{bmatrix} = 0 \tag{3.11}$$

Using equation 3.7. Due to symmetries in the permanent magnetic field, if:

$$x_m = y_m = \psi_m = \theta_m = \varphi_m = 0 \tag{3.12}$$

then:

$$F_x = F_y = \tau_\psi = \tau_\theta = \tau_\varphi = 0 \tag{3.13}$$

By also assuming the following stationary conditions:

$$\dot{x}_m = \dot{y}_m = \dot{z}_m = \dot{\psi}_m = \dot{\theta}_m = \dot{\varphi}_m = 0 \tag{3.14}$$

the only non-zero element in 3.11 is $F_z/m - g$. Given the states in equation 3.12, equation 3.14 and $u = 0, F_z$ only varies with z_m. This means that if there exist an $z_{m,eq}$ such that $F_z/m - g = 0$, then there exists an unstable equilibrium in:

$$\left.\begin{aligned} \eta_{eq} &= \Big[0, 0, z_{m,eq}, 0, 0, 0, 0, 0, 0, 0, 0, 0\Big]^T \\ u_{eq} &= \Big[0, 0, 0, 0\Big]^T \end{aligned}\right\} \quad \Rightarrow \quad \dot{\eta} = \mathbf{0} \tag{3.15}$$

Finding $z_{m,eq}$ for the system in this project was done numerically in Matlab, as explained further in section 4.6.

Chapter 4

Matlab implementation

4.1 Modelling the physical components

In order to make the Matlab model represent the physical system in a good way it was necessary to model the physical components. This was done in the most part by measuring the physical dimensions of the permanent magnets, the levitating magnet and the solenoids. In addition to this, the strength of the permanent and levitating magnets had to be estimated. As mentioned in section 3.2 the permanent neodymium magnets and the levitating magnet were modelled as solenoids with a set current. This meant finding a current such that the field strength of the modelled solenoids matched the field strength of the real magnets.
The modeling and the simulations presented in next chapters were based on the *maglevSystem*-class as in the previous project by the students of NTNU. In this thesis the Matlab files were modified in order to improve preceding results.
A GitHub repository[1] was made containing all the files used in the project.

4.2 Neodymium magnets

As the permanent magnets were grouped in stacks of three, it was natural to model one stack as one solenoid. Finding the equivalent current was done by applying the equilibrium conditions from equation 3.15 on a simplified system as shown in figure

[1] https://github.com/Nicetto/Maglev2022

4.1. The system consisted of two stacks of three neodymium magnets where one was fastened to a surface, acting as the permanent magnets, while the other stack was suspended above, acting as the levitating magnet. By measuring $z_{m,eq}$ the only unknown factor was the current needed to create the force F_z. By simulating an equivalent system in Matlab through the script "eq_curr_neo" using the parameters in table 4.1 it was possible to find the current numerically.

$z_{m,eq}$ was measured to be 7.65cm, corresponding to an equivalent solenoid current of 91.13A.

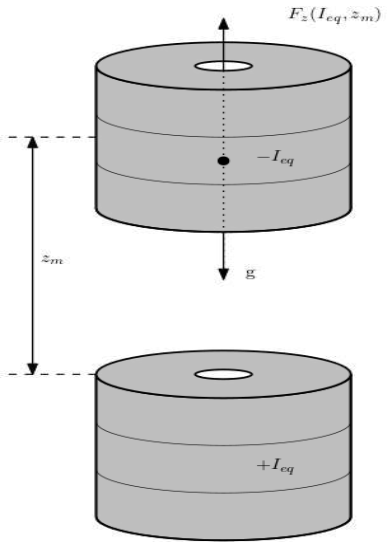

Figure 4.1: Levitating height between two stacks of neodymium magnets

Dimension	**Variable**	**Value**	**Unit**
Inner radius	ri	0.0025	m
Outer radius	ro	0.0145	m
Height	h	0.014	m
Mass	m	0.074	Kg
Number of rings in radius	nr	20	
Number of rings in height	nh	25	
Levitating height	$z_{m,eq}$	0.0765	m
Equivalent current	I	91.13	A

Table 4.1: Parameters of the neodymium magnets

4.3 Levitating magnet

The levitating magnet was modelled using the same technique as with the permanent magnets. The levitating height was measured between a stack of three neodymium magnets and the levitating magnet as there is only one levitating magnet. Since the equivalent current of a stack of three neodymium magnets was known, this could be used to find the current for the levitating magnet using the script "eq_curr_levmag". $z_{m,eq}$ was measured to be 7.40cm, corresponding to an equivalent solenoid current of 39.32A.

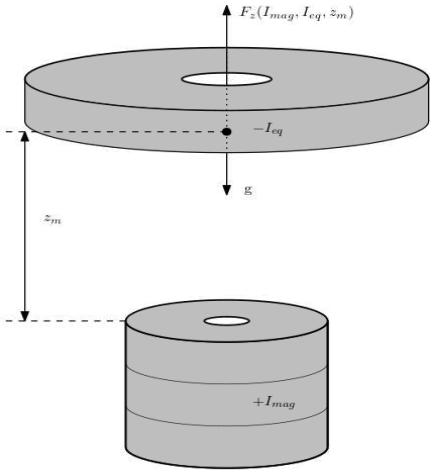

Figure 4.2: Levitating height between a stack of neodymium magnets and the levitating magnet

Dimension	Variable	Value	Unit
Inner radius	ri	0	m
Outer radius	ro	0.3	m
Height	h	0.005	m
Mass	m	0.072	Kg
Number of rings in radius	nr	20	
Number of rings in height	nh	25	
Levitating height	$z_{m,eq}$	0.074	m
Equivalent current	I	39.92	A

Table 4.2: Parameters of the levitating magnet

4.4 Solenoids

The physical dimensions of the solenoids were measured as shown in table 4.3. The maximum current through each solenoid was stated to be 0.5A.

Dimension	**Variable**	**Value**	**Unit**
Inner radius	ri	0.005	m
Outer radius	ro	0.0175	m
Height	h	0.02	m
Number of rings in radius	nr	20	
Number of rings in height	nh	50	
Offset along z-axis	z_s	0.023	m

Table 4.3: Parameters of the solenoids

4.5 Different types of simulations

The *maglevSystem*-class has two main modes of approximating the magnetic field: fast and accurate.

The fast mode models each solenoid as one discretized wire loop centered in the solenoid's mass as shown in figure 4.3. The computed force and torque are then scaled up by the number of windings in the solenoid, where $windings = nr \cdot nh$. When using the accurate mode each winding is treated as separate wire loops distributed across the volume of the solenoid, with nr concentric loops in width and nh loops in height as shown in figure 4.3. This is a more time consuming way to simulate the system as the magnetic field has to be computed separately for each winding, but it also gives a more accurate representation of the actual system given that the number of windings is set up correctly.

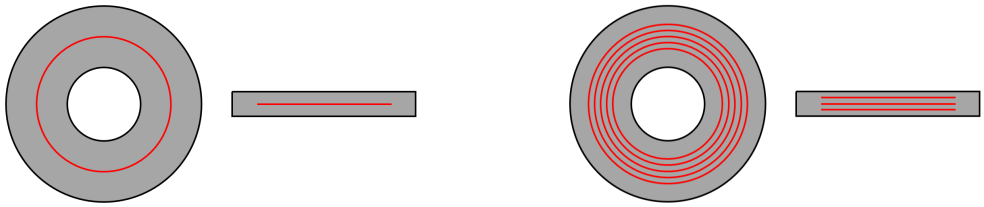

Figure 4.3: Top and side view of a solenoid modelled with the two different methods. This example has $nr = 5$ and $nh = 5$.

4.6 Equilibrium point in the simulation

As mentioned in section 4.3, the levitating magnet will be in equilibrium at a height $z_{m,eq}$ such that:

$$\frac{F_z(z_m)}{m} - g = 0 \tag{4.1}$$

Using the "z-graph" script to plot $Fz/m - g$ while varying z_m produces a plot like the one shown in figure 4.4. The equilibrium points are located where the graph equals zero. From the simulation we can state that there is a stable equilibrium point at z_m=5.91cm. It is therefore logical to choose this as the operating point for the controller.

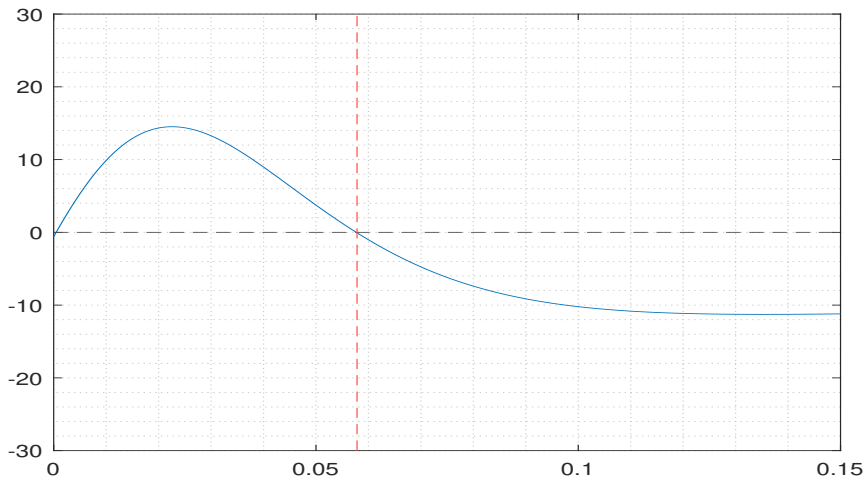

Figure 4.4: Example of a z-graph. The z-position of the levitating magnet z_m is on the x-axis

4.7 Discussion

A possible source of error could be the choice of method when finding equivalent currents for the levitating magnet and permanent magnets. The method should in theory produce a result that make the model accurately represent the actual system, but reproducing the conditions presented in equation 3.15 with accuracy is difficult with real components.

The difference between the fast and accurate simulations was bigger than expected at the start of the project. This meant that the same equivalent currents in the same solenoids gave different results depending on the simulation mode used. Slightly increasing the radius of the single wire loop used in the fast simulations (from 0.015m to 0.020m for the levitating magnet) was tried as a workaround. This gave the desired results for this specific system. However, this is not a permanent solution to the problem, as changing the system parameters most likely would require the wire loop radius to be changed again.

Chapter 5

Controller implementation and simulation

To simulate the position of the levitating magnet with respect to time, the Matlab command *ode*45 was used, exploiting the dx function in the *maglevSystem*-class.

5.1 Linear analysis

In order to make the system easier to analyse and to implement the LQR controller, it is necessary to linearise the system around the equilibrium point found in the previous chapter. The linearized system can be expressed by the following equations:

$$\begin{aligned} \eta &= A\eta + Bu \\ y &= C\eta \end{aligned} \tag{5.1}$$

The matrices A, B and C are computed by taking the partial derivatives of the existing system with respect to η and u (Andresen, Balchen and Foss 2016)[1]:

$$\dot{\eta} = f(\eta, u) \tag{5.2}$$

$$A = \begin{bmatrix} \left.\frac{\partial f}{\partial \eta_1}\right|_{(\eta_{eq}, u_{eq})} & \left.\frac{\partial f}{\partial \eta_2}\right|_{(\eta_{eq}, u_{eq})} & \cdots & \left.\frac{\partial f}{\partial \eta_{12}}\right|_{(\eta_{eq}, u_{eq})} \end{bmatrix} \tag{5.3}$$

$$B = \begin{bmatrix} \left.\frac{\partial f}{\partial u_1}\right|_{(\eta_{eq}, u_{eq})} & \left.\frac{\partial f}{\partial u_2}\right|_{(\eta_{eq}, u_{eq})} & \cdots & \left.\frac{\partial f}{\partial u_4}\right|_{(\eta_{eq}, u_{eq})} \end{bmatrix} \tag{5.4}$$

$$C = \left[\left.\frac{\partial h}{\partial \eta_1}\right|_{(\eta_{eq},u_{eq})} \quad \left.\frac{\partial h}{\partial \eta_2}\right|_{(\eta_{\text{eeq}},u_{eq})} \quad \cdots \quad \left.\frac{\partial h}{\partial \eta_{12}}\right|_{(\eta_{eq},u_{eq})} \right] \tag{5.5}$$

The partial derivatives could not be solved analytically and had to be approximated using the following finite difference approximation:

$$\frac{\partial f(\eta, u)}{\partial \eta} \approx \frac{f(\eta + \Delta, u) - f(\eta - \Delta, u)}{2\Delta} \tag{5.6}$$

Where Δ is the step size, in our case we set $\Delta = 0.0001$.

5.2 Controller design

After linearisation, remember that rotation around the z-axis can neither be observed nor controlled, so to apply the controller via the *lqr* command, it was necessary to resize the A and B matrices by omitting the rows and columns corresponding to this rotation. In this case, these are the variables φ and $\dot{\varphi}$ at positions 6 and 12. For the controller design, it is necessary to set the values of the weights of each state variable and system input. After some simulations, the best results were obtained with the following configuration, which assigns a greater weight to the x and y dimensions than to ψ and θ:

$$Q = \begin{bmatrix} 10^5 & 0 & 0 & 0 & 0 & 0 & 0 & 0 & 0 & 0 \\ 0 & 10^5 & 0 & 0 & 0 & 0 & 0 & 0 & 0 & 0 \\ 0 & 0 & 100 & 0 & 0 & 0 & 0 & 0 & 0 & 0 \\ 0 & 0 & 0 & 10 & 0 & 0 & 0 & 0 & 0 & 0 \\ 0 & 0 & 0 & 0 & 10 & 0 & 0 & 0 & 0 & 0 \\ 0 & 0 & 0 & 0 & 0 & 100 & 0 & 0 & 0 & 0 \\ 0 & 0 & 0 & 0 & 0 & 0 & 100 & 0 & 0 & 0 \\ 0 & 0 & 0 & 0 & 0 & 0 & 0 & 10 & 0 & 0 \\ 0 & 0 & 0 & 0 & 0 & 0 & 0 & 0 & 100 & 0 \\ 0 & 0 & 0 & 0 & 0 & 0 & 0 & 0 & 0 & 100 \end{bmatrix} \tag{5.7}$$

$$R = I_4 = \begin{bmatrix} 1 & 0 & 0 & 0 \\ 0 & 1 & 0 & 0 \\ 0 & 0 & 1 & 0 \\ 0 & 0 & 0 & 1 \end{bmatrix} \tag{5.8}$$

5.3 Simulation in the equilibrium point

Placing the levitating magnet with initial position corresponding to the equilibrium point the simulation returns a graph as in the figure 5.1. It is clear that the levitating magnet remains exactly in the equilibrium position. The blue line shows the trend of the z-coordinate and the red line the trend of the x- and y-coordinates.

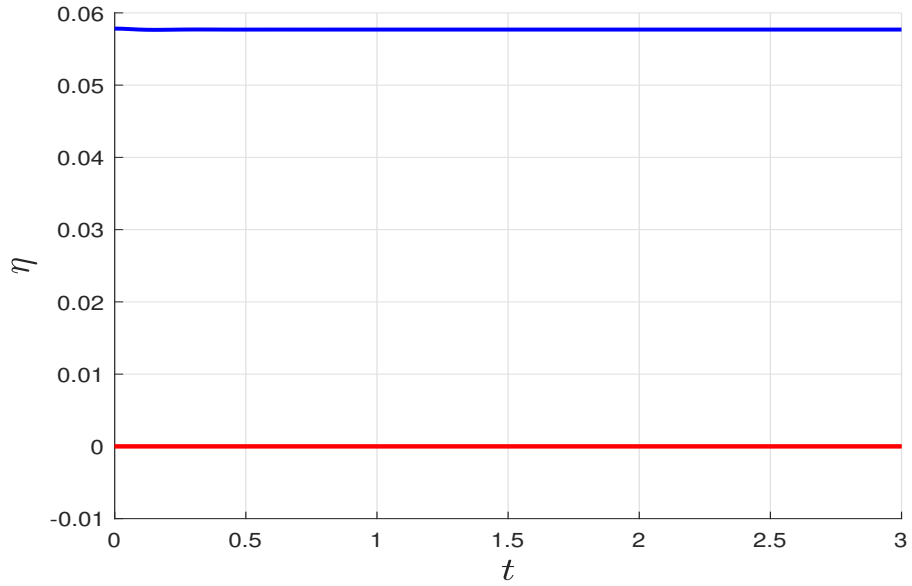

Figure 5.1: Simulation starting exactly from the equilibrium point

5.4 Simulations outside the equilibrium point

Simulating the system with the initial position of the levitating magnet (x_0) away from the equilibrium point yields different results depending on the distance between the initial point and z_{eq}.

The figures below show the simulations with starting point x_{0a} and x_{0b}, with:

$$\begin{aligned} x_{0a} &= \Big[0.001, 0, 0.001, -0.0002, 0, 0, 0, 0, 0, 0, 0, 0\Big]^T \\ x_{0b} &= \Big[0.001, 0.002, 0.002, 0, 0, 0, 0, 0, 0, 0, 0, 0\Big]^T \end{aligned} \tag{5.9}$$

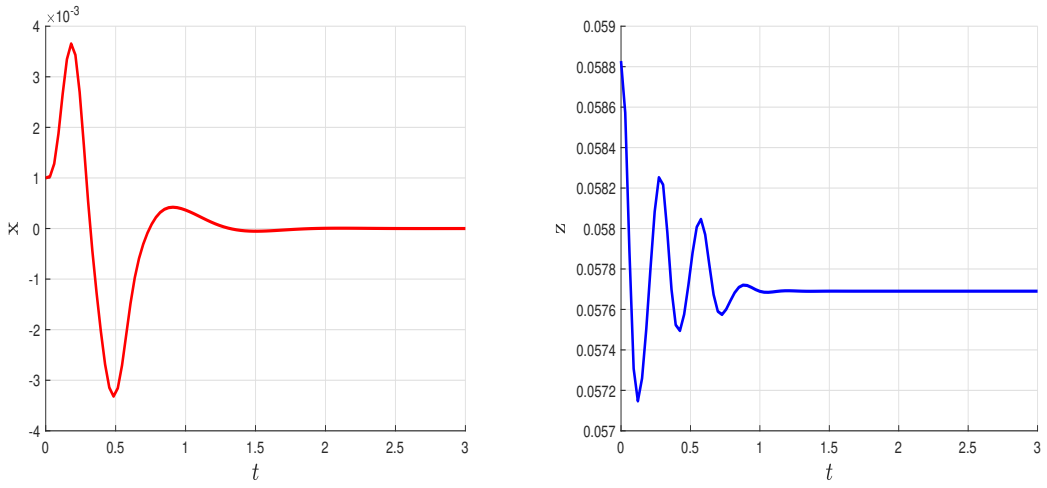

Figure 5.2: evolution of x and z coordinates from x_{0a}. The LQR controller is able to stabilize the system.

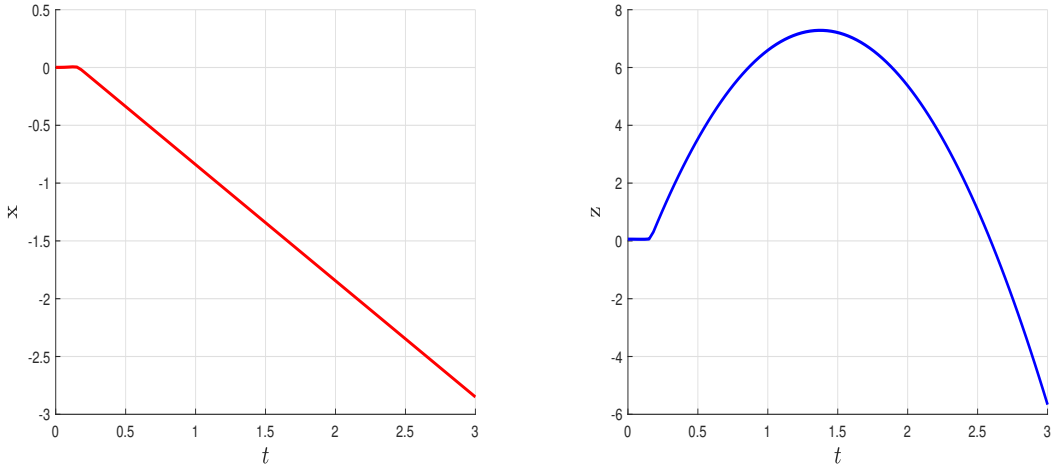

Figure 5.3: evolution of x and z coordinates from x_{0b}. The LQR controller is not able to stabilize the system.

5.5 Relation between starting distance and the maximum distance from the equilibrium

As mentioned in section 5.4, the starting point x_0 influences the final result of trajectory convergence. An attempt was made to analyse the relationship between the initial distance from equilibrium and the maximum distance achieved by $x(t)$ as the integer trajectory with respect to equilibrium. These results are shown in the following graphs:

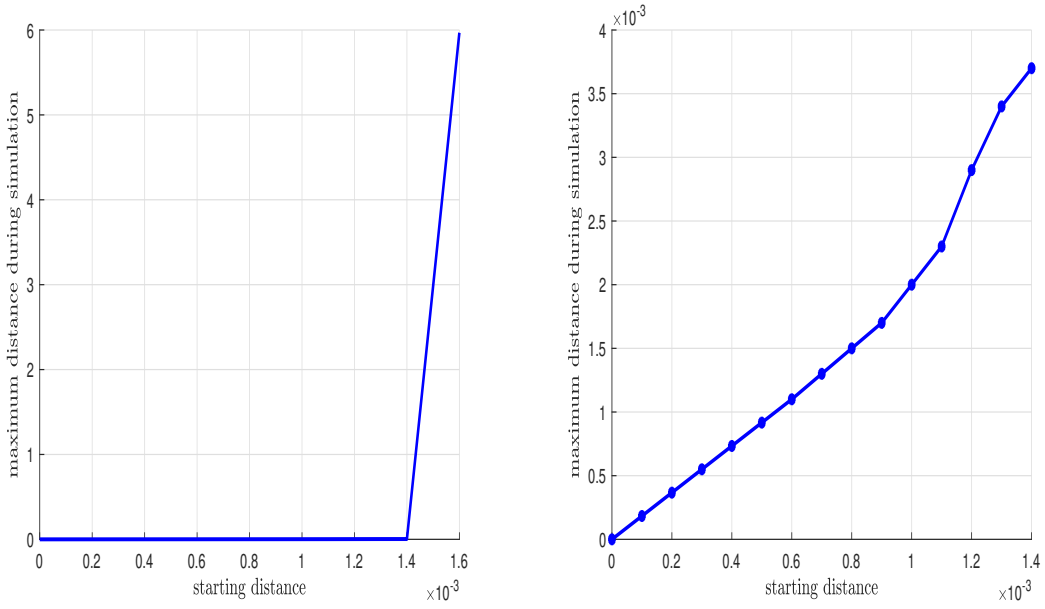

Figure 5.4: Starting distance vs maximum distance achieved during the trajectory

It is observed that the system converges to the equilibrium point when the distance between it and the starting point does not exceed 1.5mm, otherwise it diverges almost immediately. In particular, the figure on the right shows the relationship in the convergence region.

5.6 Discussion

As mentioned in section 4.7, the time difference between fast and accurate approximation is significant, the accurate simulation being much slower. This made it impossible to carry out simulations with the accurate approximation.

However, it must be emphasised that in all scripts, the fast approximation lead to numerical results that are very similar to the in the behaviour to the accurate approximation.

Chapter 6

Kalman filter implementation and simulation

The filter was also implemented on the linearized system around the equilibrium point obtained in chapter 5. Also in this case, simulations were performed using the *ode*45 command, invoked on the observations generated simulated by the h function of the *maglevSystem*-class.

6.1 Filter design

As with the controller, the filter was applied to the resized matrices mentioned in section 5.2 via the *kalman* command in Matlab.
It should be mentioned that tests on the linearised model revealed that states would not be observable with measurements from the centre alone, but it was observed that additional measurements away from the centre ensured observability. This was then implemented in the model and the real system.

To design the filter, it was necessary to set the values of the process uncertainty (Q-matrix) and measurement uncertainty (R-matrix). Due to the fact that Matlab sensors are ideal and noise-free, it was necessary to calculate the variance of sensor readings from the hardware system while holding the levitating magnet at a fixed position.

The result is that the variance of the Hall sensor measurements is approximately 0.05, therefore:

$$R\_kalman = 0.05 \cdot I_{15} \tag{6.1}$$

It is not trivial to find the optimal Q-matrix relative to our system's process, so we opted for a value much higher than R in order to improve the estimates as we already know that sensor measurements are very reliable. After a few attempts, it was decided to define Q as follows:

$$Q\_kalman = 10 \cdot I_4 \tag{6.2}$$

6.2 Filter performance

Aiming to evaluate the performance of the filter, simulations of the system were carried out with the LQR controller active in order to obtain the real trajectory of the levitating magnet and the measurements of the Hall sensors located at the centre of the platform over time. Then, by applying the Kalman filter to these newly obtained measurements, an estimate was made of the evolution of the levitating magnet's position over time. Finally, the error between the estimated and actual trajectory was computed.

Figure 6.1 shows the error in terms of spatial distance between the estimated position of the levitating magnet and its actual position starting from x_{0c}, where:

$$x_{0a} = \Big[0.0006, 0.0002, 0.0008, -0.0002, 0, 0, 0, 0, 0, 0, 0, 0\Big]^T \tag{6.3}$$

It can be appreciated that the filter estimates the trajectory very accurately after about 0.5 seconds, in fact the distance error is only significant in the first few instants of time and then decreases until it is approximately zero.

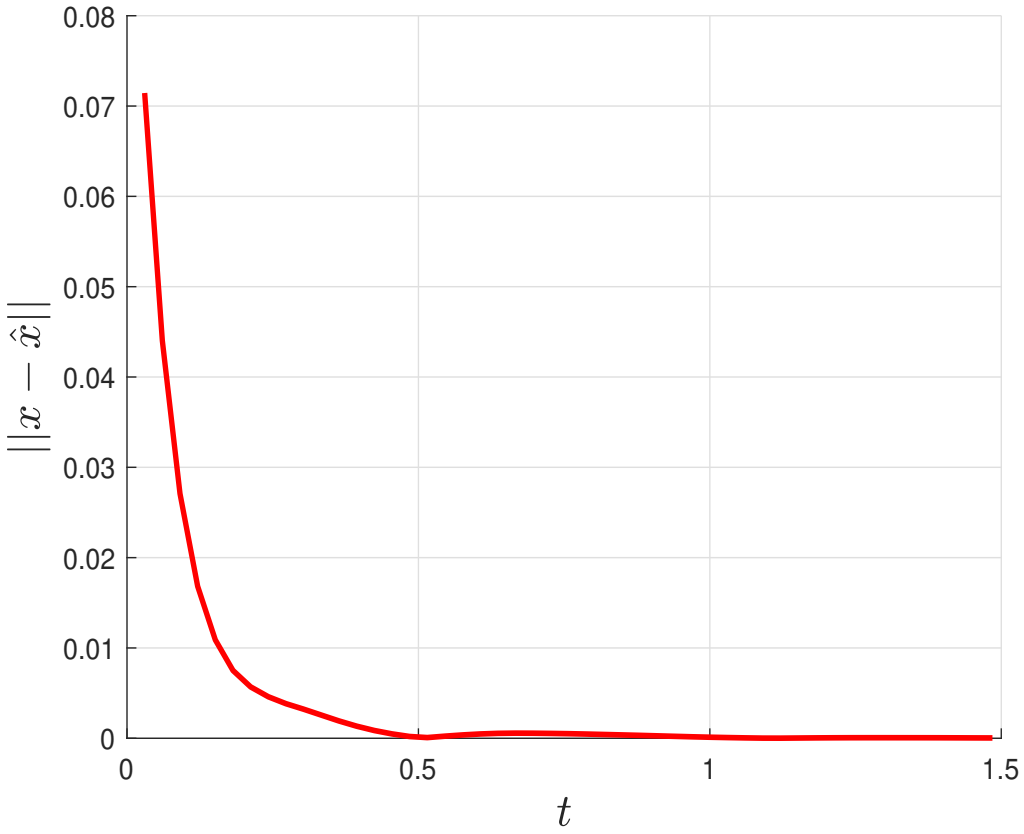

Figure 6.1: Error between the estimated trajectory and the real one

Chapter 7

Conclusions and discussion about future improvements

Considering the simulations carried out by adopting the LQR controller, it can be observed that the basin of attraction of the equilibrium appears to be much smaller than expected, in fact, as shown in section 5.5, the controller is only able to stabilise the system if the initial position of the levitating magnet is within 1.5mm of the equilibrium point. This could be due to the fact that the magnetic field around the equilibrium is not homogeneous enough due to the arrangement of the permanent magnets.

Nevertheless, I believe that, if improvements are made regarding the uniformity of the magnetic field, an LQR controller can be an effective control method to achieve a stable system.

For the Kalman filter, it seems to provide some highly accurate trajectory estimates as the estimation error clears after about 0.5s whereas the actual trajectory usually takes 1.5s to converge to the equilibrium point. Note that the Kalman filter was applied directly to the nonlinear model of the system, meaning that it would most probably be efficient if applied to the real system as well. This is promising, as the Kalman Filter could be used in conjunction with the LQR controller in order to improve the upon the current state of the art of PD control for these kinds of maglev systems (although testing on a real system remains as future work).

7.1 Future work

With regard to possible improvements to be applied in the project, it is recommended to abandon the use of the *maglevSystem*-class as it is based on the repeated invocation of the *ellipke* Matlab function, which involves a very large number of operations and consequently leads to trajectory simulations taking hours, as mentioned in section 5.6. Therefore, the creation of new Matlab functions for calculating the magnetic field and torque force is advised.

Changing the arrangement of the neodymium magnets and solenoids could be the solution to obtain a more uniform magnetic field close to the equilibrium point.

A good idea to obtain more accurate data regarding the position of the levitating magnet could be to add more Hall sensors and position them away from the centre.

Bibliography

[1] T. Andresen, J.G. Balchen, and B.A. Foss. *Reguleringsteknikk*. Institutt for teknisk kybernetikk, NTNU, 2016.

[2] Alex Becker. *Kalman Filter Tutorial*. https://www.kalmanfilter.net (Online Accessed: 02.11.2022). 2022.

[3] Anna Binnie. "Using the history of electricity and magnetism to enhance teaching". In: *Science & Education* 10.4 (2001). https://doi.org/10.1023/A:1011213519899 (Accessed: 02.11.2022).

[4] E. Bristol. "On a new measure of interaction for multivariable process control". In: *IEEE transactions on automatic control* 11.1 (1966), pp. 133–134.

[5] Chegg. *Poles Of A Magnet*. https://www.chegg.com/learn/physics/introduction-to-physics/poles-of-a-magnet (Accessed: 02.11.2022).

[6] denyssene. *Simple Kalman Filter Library*. https://github.com/denyssene/SimpleKalmanFilter (Accessed: 02.11.2022). 2020.

[7] R. Doshmanziari, H.A. Engmark, and K.T. Hoang. *Maglev model description*. https://folk.ntnu.no/hansae/Maglev_System_Description.pdf (Accessed: 02.11.2022). 2021.

[8] Ettore Fornasini. *Appunti di teoria dei sistemi*. Libreria Progetto, 2011.

[9] J. Fraden. *Handbook of Modern Science: Physics, Design and Application*. https://books.google.no/books?id=W0Emv9dAJ1kC&q=%22neodymium+magnet%22+strongest&pg=PA73&redir_esc=y#v=snippet&q=%22neodymium%20magnet%22%20strongest&f=false (Accessed: 02.11.2022). 2010.

[10] M.A. González and D.E. Cárdenas. "Analytical Expressions for the Magnetic Field Generated by a Circular Arc Filament Carrying a Direct Current". In: *IEEE Access* 9 (2020), pp. 7483–7495. DOI: 10.1109/ACCESS.2020.3044871.

[11] W Jones. "Earnshaw's theorem and the stability of matter". In: *European Journal of Physics* 1.2 (Apr. 1980), 85–88. https://doi.org/10.1088/0143-0807/1/2/004 (Accessed: 20.10.22). DOI: 10.1088/0143-0807/1/2/004. URL: https://doi.org/10.1088/0143-0807/1/2/004.

[12] rlabbe. *Kalman and Bayesian Filters Library*. https://github.com/rlabbe/Kalman-and-Bayesian-Filters-in-Python (Accessed: 02.11.2022). 2022.

[13] D. E. Seborg et al. *Process Dynamics and Control*. Wiley, 2016, pp. 331–338.

[14] S. Skogestad and I. Postlethwaite. *Multivariable Feedback Control*. Wiley, 2007.

[15] Zhong Jian Wang and Yong Ren. "Magnetic Force and Torque Calculation Between Circular Coils With Nonparallel Axes". In: *IEEE Transactions on Applied Superconductivity* 24.4 (Aug. 2014). DOI: 10.1109/TASC.2014.2311412.

[16] Wikipedia contributors. *Magnetic levitation — Wikipedia, The Free Encyclopedia*. (Accessed 2-November-2022). 2022. URL: https://en.wikipedia.org/w/index.php?title=Magnetic_levitation&oldid=1112700831.

[17] Hamid Yaghoubi. "The most important maglev applications". In: *Journal of Engineering* 2013 (2013). https://www.hindawi.com/journals/je/2013/537986/ (Accessed: 02.11.2022).